BBC RD 1976/21

BBC • IBA

Engineering Research Report

The work covered by this report was undertaken by the BBC Research Department for the BBC and the IBA

A circularly-polarised aerial for satellite reception

C. Gandy, B.Sc.

Research Department, Engineering Division
THE BRITISH BROADCASTING CORPORATION   August 1976

BBC RD 1976/21
UDC 621.396.677.7
621.396.946

A CIRCULARLY-POLARISED AERIAL FOR SATELLITE RECEPTION

C. Gandy, B.Sc.

Summary

A circularly-polarised feed aerial for a 2·44m parabolic reflector was designed and constructed to form the basis of a satellite receiving station. Waveguide components and a hybrid-mode scalar-horn aerial were used, with a facility for the reception of either sense of polarisation. The cross-polar isolation was found to be 30 dB, and with a 2·44 metre parabolic reflector the aerial gain was estimated to be 40 dB, the efficiency approaching 70%.

Issued under the authority of

G D Monteath

Head of Research Department

Research Department, Engineering Division,
BRITISH BROADCASTING CORPORATION

August 1976

(RA-148)

A CIRCULARLY-POLARISED AERIAL FOR SATELLITE RECEPTION

A CIRCULARLY-POLARISED AERIAL FOR SATELLITE RECEPTION

C. Gandy, B.Sc.

1. Introduction

In June 1977 the Orbital Test Satellite (OTS) will be launched into geo-stationary orbit in preparation for a series of propagation tests.[1] The down-link will be circularly-polarised, with a frequency of about 12GHz. In addition to unmodulated pilot signals it is hoped that television and multiplexed sound signals will be radiated.

A satellite receiving station is being planned for Research Department and the aerial described in the Report was designed for this purpose.

To save time and expense a surplus 2·44 metre parabolic dish reflector was acquired to form the basis of the receiving aerial. The Report describes in detail the design and construction of a circularly-polarised feed aerial to be mounted at the focus of this reflector.

The aims of the design were:

(a) to illuminate the available reflector as efficiently as possible consistent with low sidelobe levels.

(b) to maintain a large degree of isolation between the two possible polarisations whilst providing an output signal in standard waveguide for either polarisation.

The final design fulfills both of these criteria as a feed alone, but further work on the attachment of the feed to the reflector will be needed before numerical results for the complete aerial can be presented. However, reasonable predictions can be made[2] from a knowledge of the feed pattern.

2. Description of the feed system

The circularly-polarised feed system is shown in Fig. 1. The hybrid-mode feed aerial is a scalar horn with a flare angle of 90°.[3,4] It has a −10 dB half beamwidth of 65° in both E and H planes to give a maximum aperture efficiency of 83% when combined with a parabolic reflector with a focal length to diameter (f/D) ratio of 0·5. This corresponds to a gain of 48 dB (relative to an isotropic source*) with the reflector in use. Fig. 2 shows the corrugations[5] on the surface of the flare which form an impedance boundary affecting the E and H fields similarly.[3] The result is a hybrid-mode of propagation (HE_{11}), possessing cylindrical symmetry about the axis of the aerial. This feature maximises the efficiency of the reflector-feed system. Hybrid-mode feeds are noted for their suppression of rear and side lobes.[6]

The circularly-polarised signal is passed to the circular polariser in circular waveguide, using the dominant TE_{11} mode.[7,8,9] The circular polariser shown in Fig. 3 is birefringent to orthogonal TE modes and consists of a series of reactive probes in a circular waveguide.[10,11,12,13,14] It reverses the phase conditions for a circularly polarised wave[15] and converts it to linear polarisation, vertical for one sense of rotation and horizontal for another.

The orthogonal mode coupler shown in Fig. 4 separates the two linear polarisations[16,17] by making use of their orthogonality and provides two isolated outputs, one in rectangular waveguide, in the dominant TE_{10}

* All gains in the report are relative to an isotropic source.

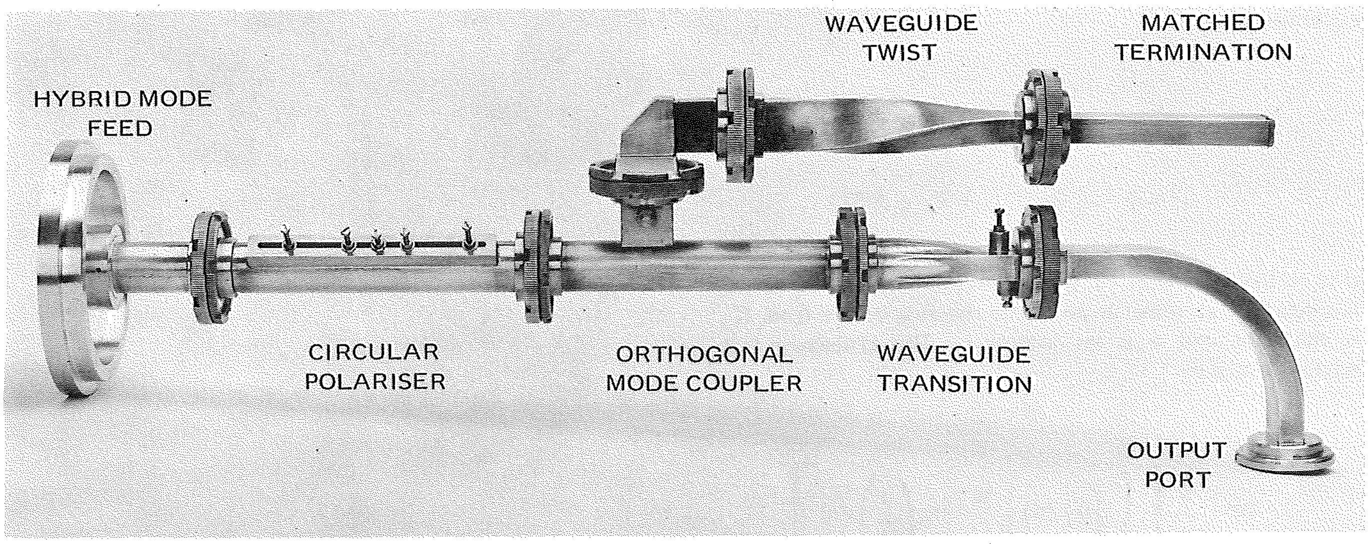

Fig. 1 - Circularly-polarised feed system

mode[18,19] and one in circular waveguide. The latter is converted to rectangular guide by the waveguide transition[20] shown in Fig. 5. This component makes use of a smooth taper to convert the modes TE_{11} to TE_{10}.

Mismatches in the orthogonal mode coupler are tuned out by screw tuners,[21] with λ/8 spacing and adjustable penetration, on each of the rectangular guide output ports.

By means of a right angle corner[22] and a waveguide twist[23] the sidearm port of the coupler is brought out parallel with the collinear port, as shown in Fig. 1. This allows connection to either port using an E-plane bend and a short length of flexible waveguide,[24] for the reception of circular polarisation of either sense. The unused port is terminated with a matched load, containing an iron-loaded resistive structure.

A glass-fibre housing has been designed for the feed incorporating brackets for the attachment of support legs to hold it at the focus of the dish reflector. An air pressurising system has also been designed to prevent the ingress of moisture when the aerial is finally located out-of-doors.

3. The design of the feed system

3.1. Hybrid-mode feed aerial

By measurement of the diameter and depth (aperture to vertex) of the parabolic dish it was found to have a f/D ratio of 0·5 and hence an angular aperture (ψ) of 56·85°: see Fig. 6. A Cassegrain system[25,26,27,28,29] was ruled out because a subreflector could not be manufactured accurately enough in the time available, so a front feed was decided upon. The efficiency of a front fed system is largely dependent on the distribution of available illumination power over the aperture. Generally the radiation pattern of a feed can be represented by the equation (2):

$$G_f(\psi) = G_o(n) \cos^n \psi, \quad 0 \leqq \psi \leqq \pi/2$$

$$= 0 \qquad , \qquad \psi > \pi/2$$

over a large portion of the main lobe, where G_f is the illumination at some angle ψ off the axis of the feed, G_o is the gain and n is an integer. The efficiency ξ is related to this by

$$\xi = \cot^2 \frac{\psi}{2} \left[\int_o^{\psi} \left[G_f(\psi) \right]^{1/2} \tan \left(\frac{\psi}{2} \right) d\,\psi \right]^2$$

The integral of power radiated by the feed over all angles (in a sphere) is equal to that of an isotropic radiator, so

$$\int_o^{\pi} \left[G_f(\psi) \right] 2\,\pi\,R^2 . \sin \psi . d\,\psi = 4\,\pi\,R^2$$

Where $2\pi R^2 . \sin \psi . d\psi$ is the element of area on a sphere of radius R, centred on the feed, and $4\pi R^2$ is the total surface area of the sphere. This gives

$$G_o(n) = 2(n+1) \qquad \text{. . . so by substitution}$$

$$\xi = 2(n+1) \left[\cot \frac{\psi}{2} \int_o^{\psi} \cos^{n/2} \psi \tan \left(\frac{\psi}{2} \right) d\,\psi \right]^2$$

This expression has an explicit solution for even values of n and some of these are shown graphically in Fig. 7. From these curves it can be seen that for a value of

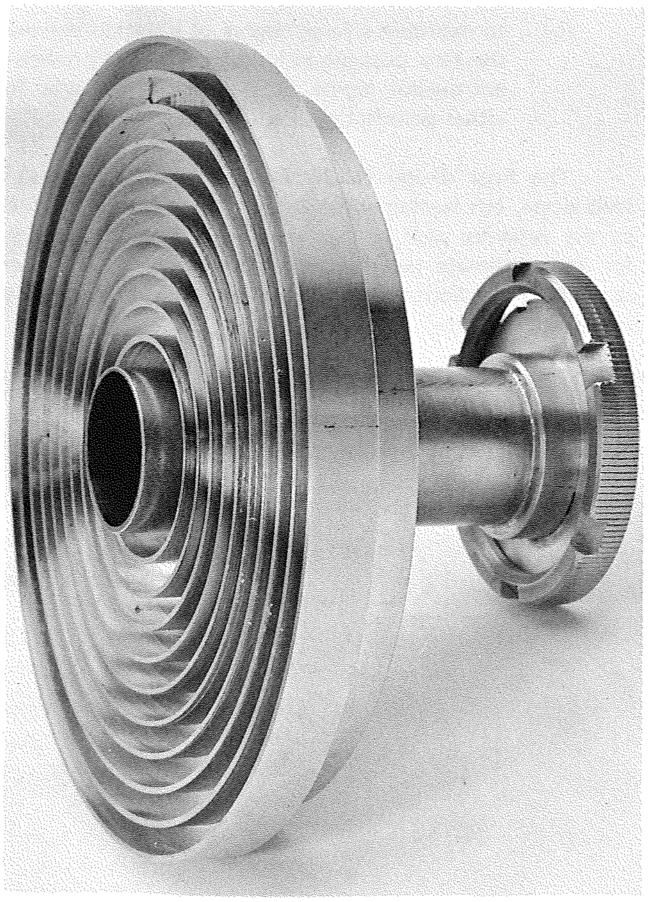

Fig. 2 - Hybrid-mode feed aerial

ψ = 56·85°, for a maximum efficiency of 0·83 the required value of n is about 4. The required feed pattern can then be represented by

$$G_f\ (\psi) = 10 \cos^4 \psi, \quad 0 \leqq \psi \leqq \pi/2$$
$$= 0 \qquad , \quad \psi > \pi/2$$

This implies a gain G_o of 10 dB for the feed, and a −10 dB half-beamwidth of 55·78°. However, the space attenuation factor A[30] must be subtracted from these figures to give their true values

$$A = -20 \log \frac{R}{f} = -20 \log \sec^2 \frac{\psi}{2}$$

$\therefore A = -2{\cdot}23$ dB at the rim of the reflector.

So the −7·77 dB half-beamwidth is 55·78°, or in other words the −10 dB half-beamwidth is 63·28°.

The specification for the feed aerial can be written as

Gain $\approx$ 10 dB

−10 dB half-beamwidth = 63·28°

Feed illumination pattern (taper) ... $\cos^4$

Such a pattern is illustrated in Fig. 8. Any departure from these figures will tend to reduce the performance. If the feed beamwidth is increased, a larger area of the aperture will be illuminated uniformly so the gain will be increased, but the spillover introduced will increase the noise temperature of the aerial system. Conversely, if the feed beamwidth is reduced, the sidelobe and spillover levels will drop, but so will the gain because a smaller area of the aperture will be illuminated uniformly.

The gain of the reflector-feed aerial is given by

$$G_A = \xi \left(\frac{\pi D}{\lambda}\right)^2$$

= 48·6 dB with the calculated value of ξ at λ = 2·58 cm, the wavelength corresponding to the design frequency of 11·6GHz.

The feed aerial required to suit the above specification has to be cylindrically symmetrical because circular-polarisation is to be used. Although pyramidal horns with twisted throats have been used,[31] these are difficult to construct and rather inflexible in use.

The first obvious choice was a conical horn[32,33] but for the beamwidth required this would have been very lossy, approximating to a circular waveguide beyond

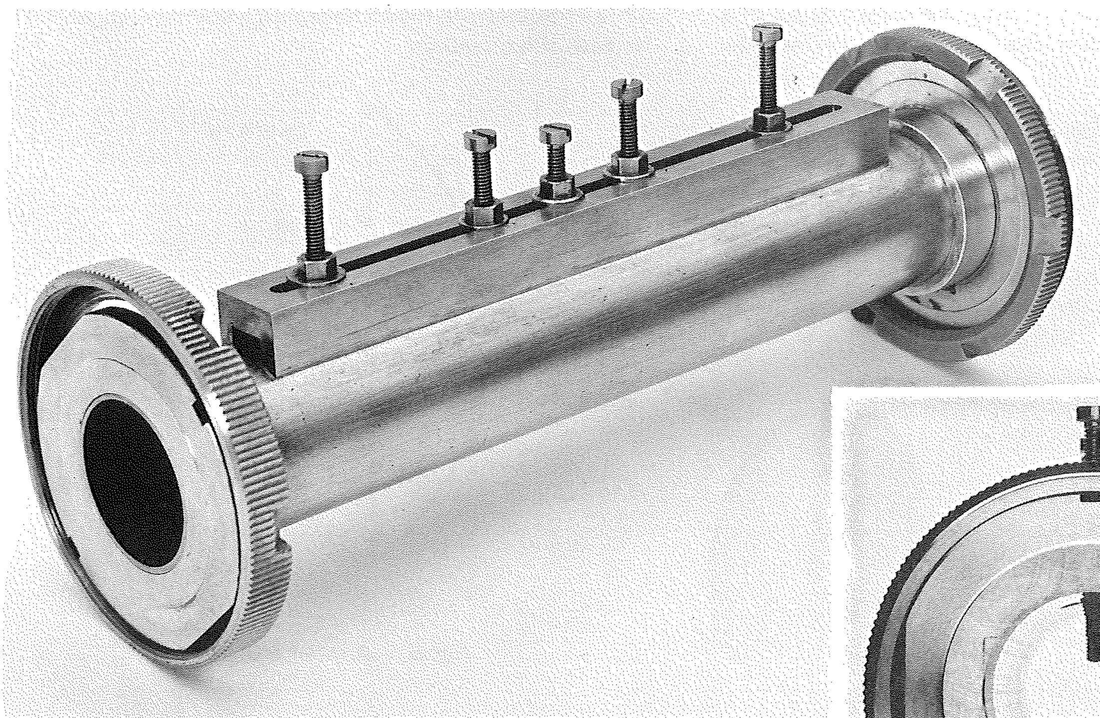

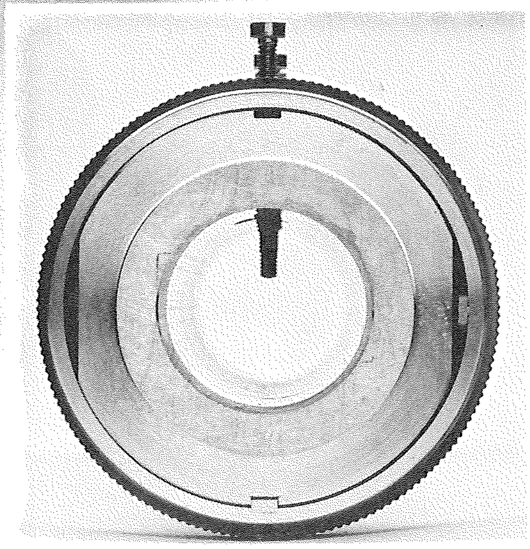

Fig. 3 - Circular polariser

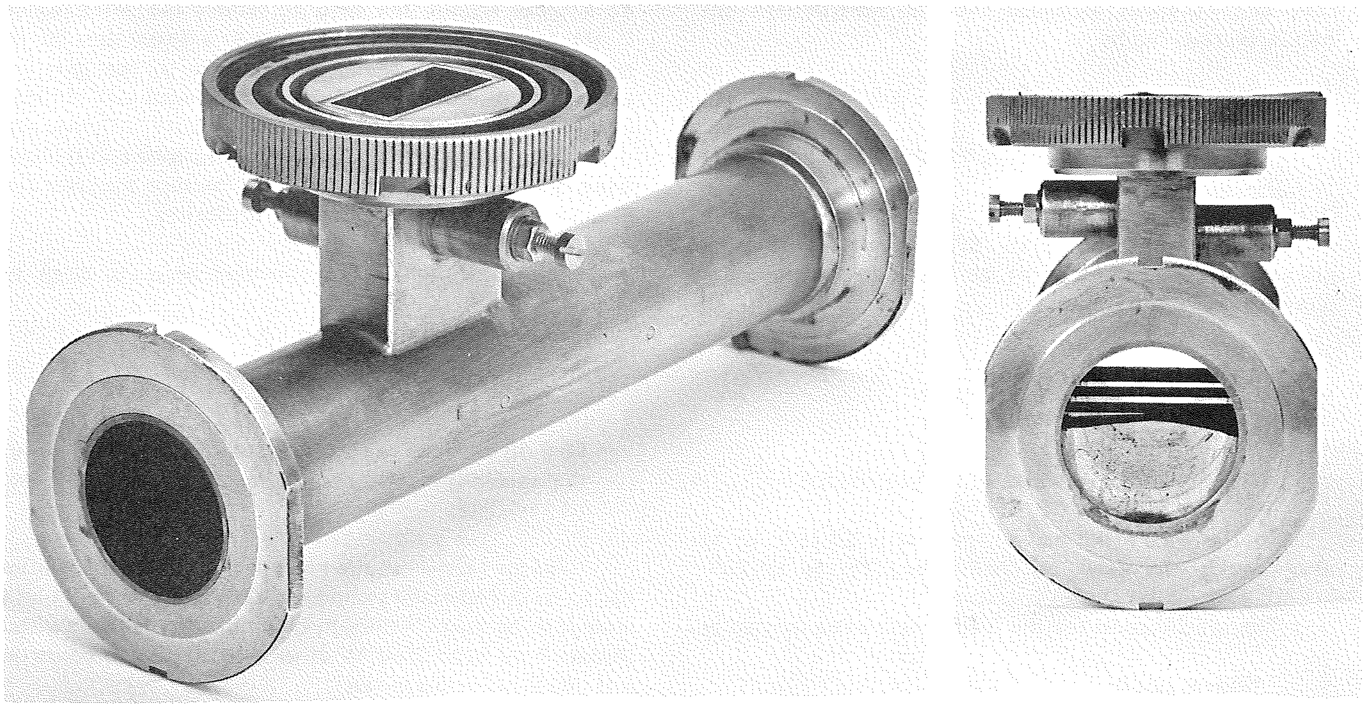

Fig. 4 - Orthogonal mode coupler

cutoff.[34] The axial mode helix[35] and the Cutler feed[36] were also investigated, but the former was found to be very lossy at the wavelength in use, and the latter would have fed the dish reflector from a ring focus instead of a point. Defocussing the feed generally increases the sidelobe level.[37]

A more recent type of feed, which was eminently suited to this application was the hybrid-mode scalar feed,[3,4] which takes the form of a corrugated conical horn, fed by a circular waveguide. Fed at the apex of the flare the −10 dB half beamwidth has been found to be approximately ¾ the flare angle, and this is not so dependant on the diameter of the mouth of the horn as in the case of a simple, diffraction limited conical horn. By feeding the horn from a point other than the apex the ratio can be modified, thus it is possible to get the required 63° half-beamwidth from a horn with a 90° flare angle[38,39] for ease of fabrication.

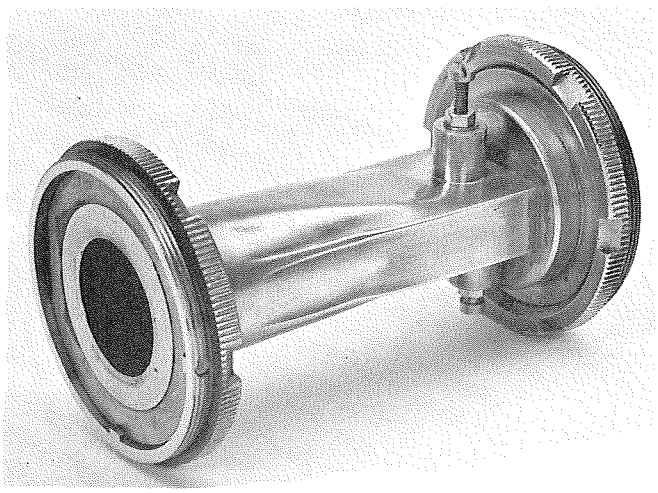

Fig. 5 - Waveguide transition

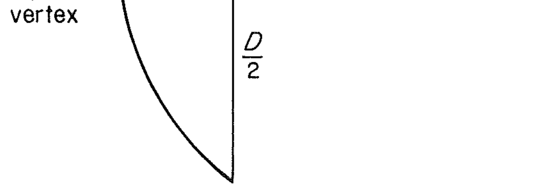

Fig. 6 - Angular aperture

Texts on the theory of scalar feeds[40,41] point out that the corrugations on the surface of the flare present a reactive boundary which approaches the same boundary conditions for TE and TM waves at grazing incidence. If the corrugations are made deep enough so that the reactance is capacitive, surface waves are not supported and a hybrid-mode, HE_{11} spherical wavefront results. The

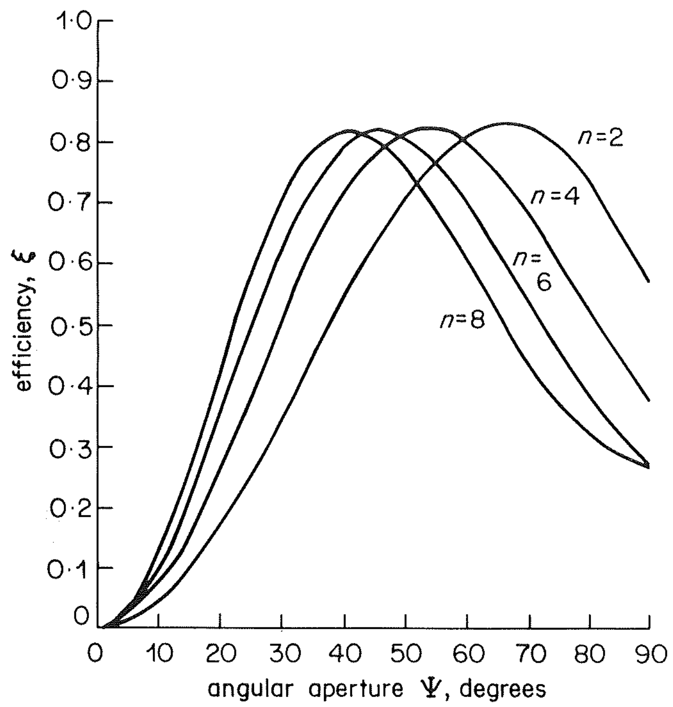

Fig. 7 - Dependence of efficiency on angular aperture and illumination pattern

HE_{11} mode is composed of both TE_{11} and TM_{11} modes.

The design of a scalar feed for this application reduces to providing a corrugated flare of at least 2λ length, with corrugations of depth greater than λ/4*, spaced by very thin ridges, at least 3 per wavelength along the flare, and the provision of an adjustable feed point for the circular waveguide.

Fig. 9 shows the construction of the feed aerial, employing a flare length of 2·2λ with 5 corrugations per wavelength. The depth of the corrugations is increased towards the feed point in an attempt to improve the match to the waveguide which, as Fig. 2 shows, projects forward beyond the apex of the flare. This projection was adjusted on test to give the required beamwidth.

3.2. Circular polariser

A circularly polarised wave of amplitude E can be represented by a pair of linearly polarised waves in time and space quadrature, thus;

$$E_x = \frac{1}{\sqrt{2}} E \sin \omega t; \quad E_y = \frac{1}{\sqrt{2}} E \cos \omega t$$

If these are subjected to a phase shift such that,

$$E_x = \frac{1}{\sqrt{2}} E \sin (\omega t - \phi_x); \quad E_y = \frac{1}{\sqrt{2}} E \cos (\omega t - \phi_y)$$

with the condition that $\phi_y - \phi_x = \pi/2$

then $E_x = \frac{1}{\sqrt{2}} E \sin (\omega t - \phi_x)$; $E_y = \frac{1}{\sqrt{2}} E \sin (\omega t - \phi_x)$.

Taking the resultant at $\pi/4$ in space to each of the original waves;

$$E_{(x,y)} = E \sin (\omega t - \phi_x)$$

which is a linearly polarised wave.

The sense of rotation (clockwise/anti-clockwise) of the circularly polarised wave determines which plane this resultant will lie in. Therefore the circular polariser (or de-polariser in this case) must consist of a bi-refringent phase shifter, in circular waveguide. A capacitive post[10,11] entering through the wall of the waveguide will produce such a phase shift, but one alone would introduce a serious mismatch if $\pi/2$ phase shift was to be produced at a point. A series of posts spaced along the length of the guide with a binomial distribution of penetrations[42] will produce an impedance transformation which will minimise reflections. In this case the $\pi/2$ phase shift will be made up in steps.

The final form of the design used is shown in Fig. 10. The spacing and penetration of the posts (6BA screws) was adjusted on test to give the best axial ratio (ratio of $|E_y| : |E_x|$) consistent with a good match for a linearly-polarised input signal in the TE_{11} mode, aligned with the E plane at 45° to the plane of the

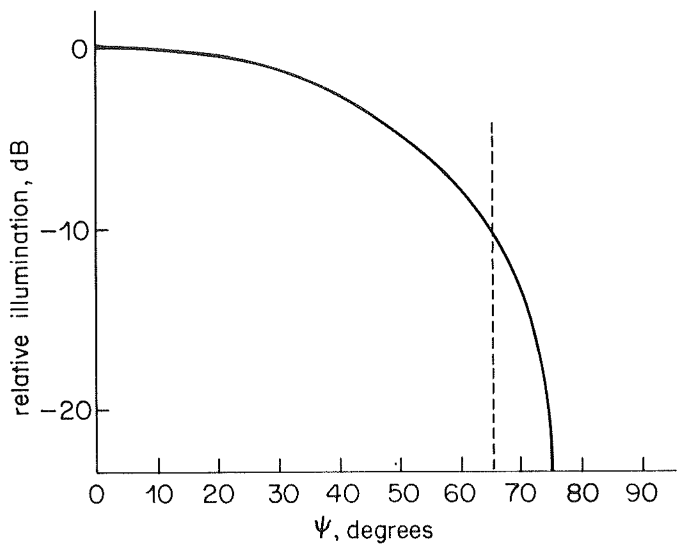

Fig. 8 - Aperture illumination taper

* But less than λ/2. About 0·3λ is found to give good axial symmetry.[5]

posts.

3.3. Orthogonal mode coupler

It has been shown that the polariser converts circularly-polarised waves of opposite rotation senses into linearly-polarised waves of orthogonal polarisations. It was therefore necessary to separate the orthogonal polarisations (TE_{11} modes) in order to select which circular polarisation was to be received. This process was achieved with the orthogonal mode coupler shown in Fig. 11. The main design problem was to ensure a large degree of isolation between the output ports consistent with a good match.

The vertically polarised mode travels through the circular waveguide section with little attenuation or reflection because all the obstructions in this section are thin, conductive and in the H-plane. Loss through the sidearm is minimised by the inclusion of a pair of parallel plates in a frame, supported in the aperture of the rectangular section. These plates preserve the continuity of the wall of the circular guide for the surface currents of a vertically polarised TE_{11} mode.

Passing through the circular section, the vertically-polarised mode is coupled to a standard rectangular waveguide by the waveguide transition.

The horizontally-polarised mode entering the coupler can pass into the sidearm without loss because the parallel plates at the aperture are now orthogonal to the E-plane. Furthermore, propagation along the circular section beyond this aperture is prevented by a series of horizontal inductive rods with varying spacing. These provide almost total reflection, and their positions were found experimentally, aiming for good isolation consistent with a good match at the input port. For convenience the sidearm was made of standard rectangular waveguide (WG16). Coupling to the sidearm introduces a simple TE_{11} to TE_{01} mode conversion, whilst the waveguide transition on the other output port introduces a TE_{11} to TE_{10} conversion. The TE_{01} mode from the sidearm was converted to TE_{10} by the use of a 90^{o} waveguide twist.

Both output ports of the coupler were tuned using $\lambda/8$ spaced screw-tuners[21] in order to reduce mismatch. This method of matching was found adequate for the bandwidth required.

A carbon loaded vane was placed in the output end of the circular section to absorb any horizontally polarised modes produced by the transition due to mechanical

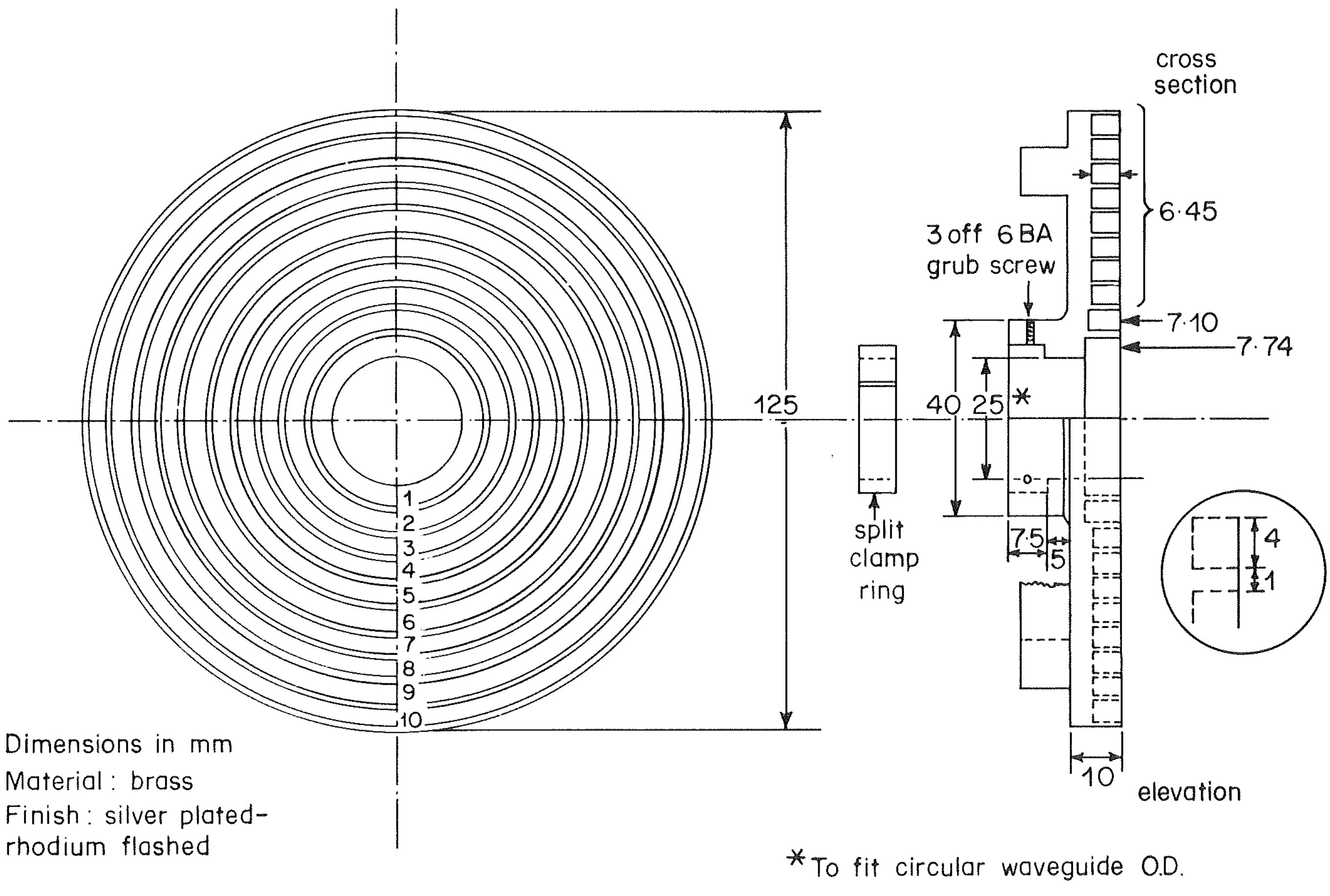

Fig. 9 - Hybrid-mode feed aerial

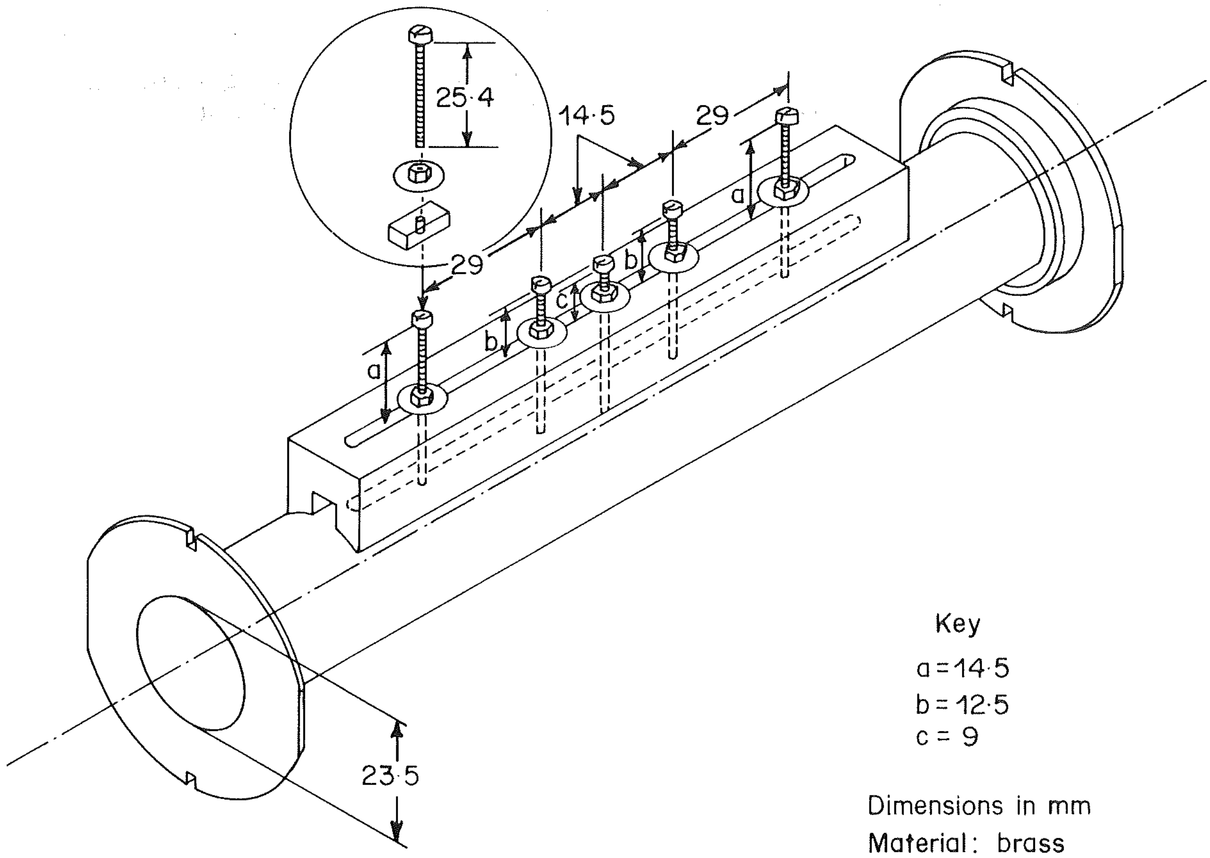

Fig. 10 - Circular polariser

mis-alignment.

3.4. Weatherproofing

A glass-fibre housing was designed for the feed, with airtight glands at the waveguide and aerial ends. Mounting lugs were built into this housing. The aerial was silver-plated and rhodium-flashed since the construction of a radome was impractical. To air-seal the aerial, a polystyrene window[47] was made, $\lambda/2$ thick, to fit into the circular waveguide, and all waveguide connections were fitted with rubber "O" rings. A small compressed air system was then constructed to keep the pressure in the system about 48 $kN.m^{-2}$ higher than atmospheric.

4. Results

4.1. The aerial

The hybrid-mode feed aerial was connected directly to the transition and fed to a detector in standard rectangular waveguide. This assembly was mounted on a turntable in the centre of a large laboratory and a horn aerial radiating an 11·6GHz linearly-polarised signal was mounted 7 metres away. Fig. 12 shows the E-plane radiation pattern that was obtained after adjustment of the feed waveguide projection. There is a close agreement with the required ($\cos^4 \psi - A$) curve. Fig. 13 shows the H-plane pattern which to ±½ dB is identical. The bump at 98° has since been found to be a room reflection and it is hoped that further tests in an anechoic environment will show a much reduced sidelobe level. By varying the waveguide projection over 5mm some 20° of variation in the position of the −10 dB point was possible. At the position chosen, the −10 dB point occurred at 65° instead of 63°, but the match was slightly improved.

Using a slotted line the reflection coefficient of the aerial and transition together was found to be 0·08 and inductive.

4.2. The polariser

The circular polariser was coupled to a simple conical horn aerial and fed through the transition by a signal in standard rectangular waveguide. By fine adjustment of the posts an axial ratio of 0·5 dB was obtained, sensing the radiation from the horn with a linearly polarised receiver. This necessarily required a good match because the transition was found to be highly reflective to the orthogonal polarisation (for which the rectangular guide would have been into far cut-off). A reflection coefficient of 0·01 was obtained for the polariser and transition when feeding

an area of "Spacecloth" through the horn.

4.3. The coupler

The orthogonal mode coupler was first tested through the circular section, with an identical transition at each end. The reflection coefficient could be tuned to less than 0·01 and the isolation to the sidearm was well in excess of 40 dB (immeasurable with the instruments available). The sidearm was then driven and a reflection coefficient of 0·02 was obtained. This figure is understandably higher because the mode conversion involved in this case is much more abrupt. The isolation to the other output port was again in excess of 40 dB.

4.4. The complete system

The feed system was assembled as shown in Fig. 1 with a matched termination at each output port in turn. The polariser was aligned for clockwise polarisation (looking at the aerial) when the sidearm of the coupler was fed, and anti-clockwise polarisation with the collinear path was fed.

Final adjustment yielded the following figures at 11·6GHz:

Axial ratio (clockwise)	0·5 dB
Axial ratio (anti-clockwise)	0·6 dB

Output port reflection coefficient (clockwise) 0.11
Output port reflection coefficient (anti-clockwise) 0.10

Cross polar isolation (calculated: see Appendix 1)

(clockwise)	30 dB
(anti-clockwise)	30 dB

Cross polar isolation (measured using helices of opposite rotation with a known 40 dB isolation)

(clockwise)	28 dB
(anti-clockwise)	29 dB

The transmistion 3 dB bandwidth was measured as 200 MHz, i.e. the band limits were approximately 11·5GHz and 11·7GHz.

4.5. Further tests

Time and instruments were not available for tests of axial ratio off the boresight, efficiency when feeding the parabolic reflector and the final reflector-feed aerial radiation pattern, but it is hoped that these will be reported in full at a later date, when mounting and steering assem-

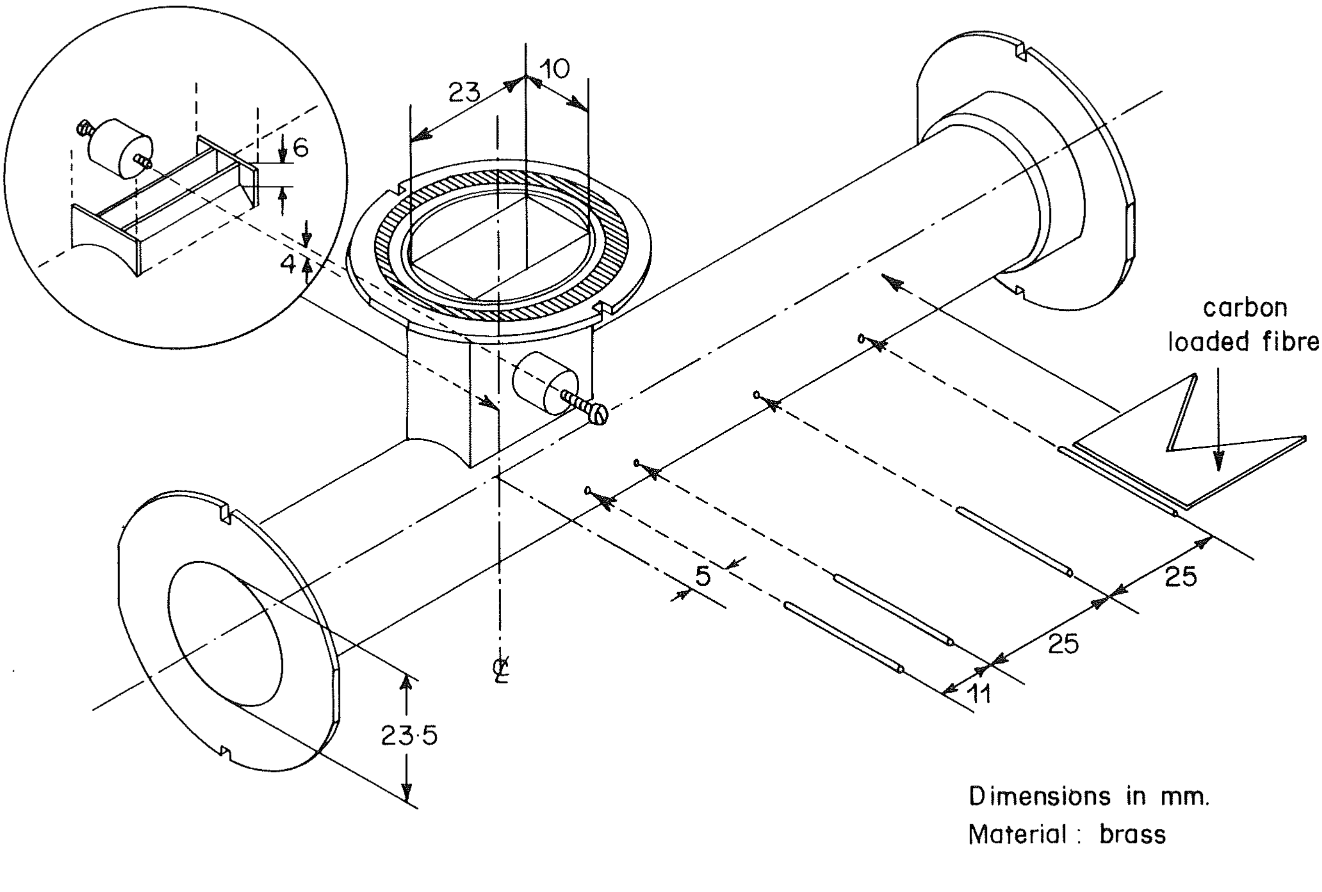

Fig. 11 - Orthogonal mode coupler

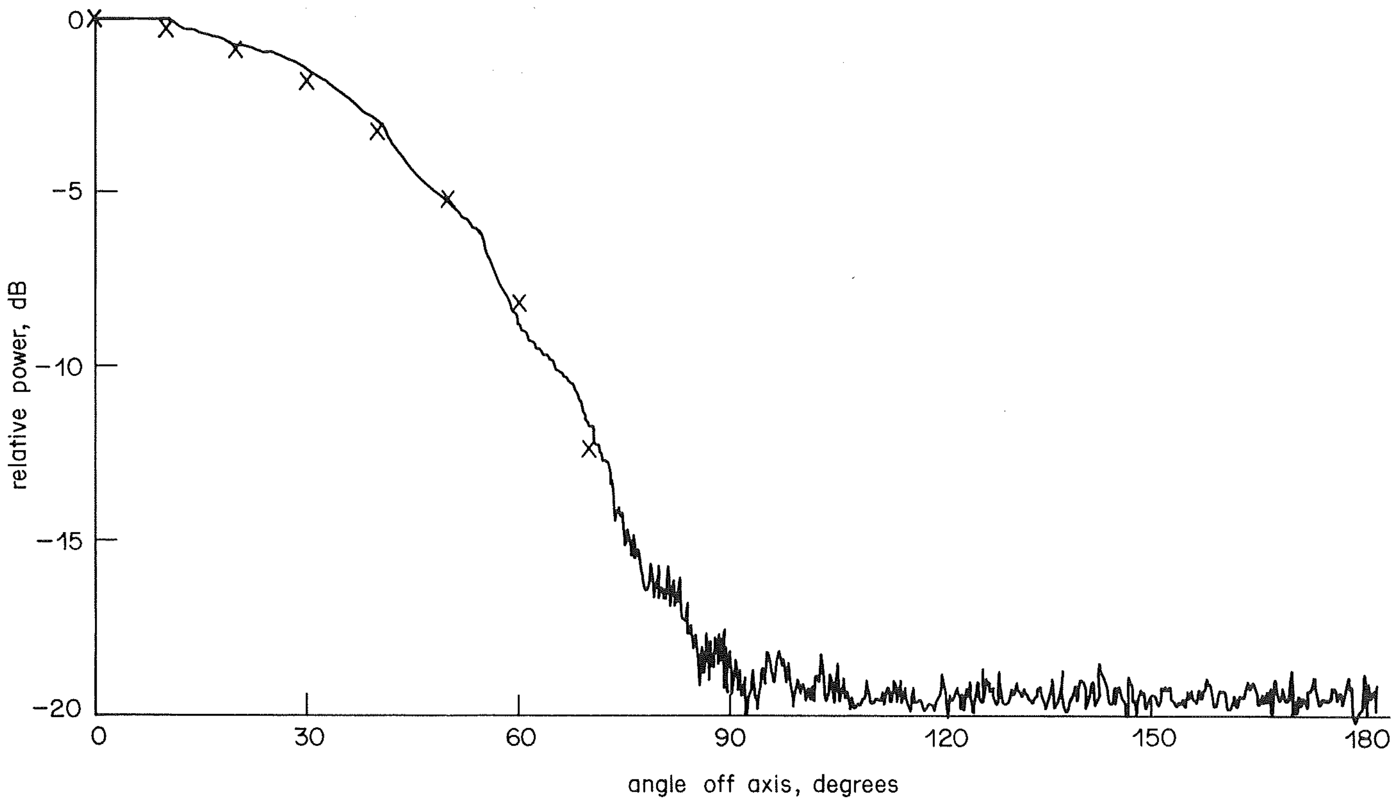

Fig. 12 - Feed aerial radiation pattern — E plane

= measured pattern x———x = $(\cos^4 \psi - A)$ calculated

blies have been constructed.

5. Conclusions

A circularly-polarised feed aerial system has been designed and constructed for a parabolic reflector of given dimensions. The results obtained were encouraging and should lead to the production of a high-quality satellite receiving station. Much mechanical work remains to be done before the aerial system will be complete, but predictions[43] can be made on its performance using the available data.

Using glass-fibre support struts (3 off) to hold the feed at the focus of the reflector it is estimated that the overall efficiency will approach 70%, with a corresponding gain of 40 dB. The reflection coefficient at the output port may be improved by as much as 2 dB by the use of vertex-plate matching techniques.[44] The cross-polar isolation of the complete aerial will be degraded by inaccuracies in focal positioning[45] but a figure of 25 dB should be obtainable over a sizeable portion of the main lobe.

It has been shown that the construction of such a feed system is possible without the expense of electroforming and similar techniques, but no doubt the results obtained could be improved upon. However, it is heartening to note that a similar feed system[46] constructed by RCA gave comparable results.

6. References

1. European Space Research Organisation. 1975. Communications Satellite Program; the orbital test satellite. Data Book, Issue 2.

2. SILVER, S. 1949. Microwave Antenna Theory and Design, pp. 424-427. McGraw-Hill, 1949.

3. SIMMONS, A.J. *and* KAY, A.F. 1966. Design and Construction of Large Steerable Aerials. The Scalar Feed: a high performance feed for large parabolic reflectors. IEE Conference Publication No. 21.

4. CLARRICOATS, P.J.B. *and* SAHA, P.K. 1970. Earth Station Technology. Scalar feeds for earth station antennas. IEE Conference Publication No. 72, pp. 240-244.

5. McINNES, P.A. *and* DOCKER, D.D. 1971. Corrugated horns with very wide flare angle. Proc. 2nd European Microwave Conference, Stockholm, pp. B7/2:1 - B6/5:4.

6. JEUKEN, M.E.J. *and* LAMBRECHTSE, C.W. 1971. Difference modes in the scalar feed. Proc. 2nd European Microwave Conference, Stockholm, pp. B6/5:1 - B6/5:4.

7. SILVER, S. Ibid. pp. 233-235.

8. RAGAN, G.L. 1948. Microwave Transmission

Circuits. pp. 54-55. McGraw-Hill, 1948.

9. MARCUTITZ, N. 1951. Waveguide Handbook. pp. 66-72. McGraw-Hill, 1951.

10. RAGAN, G.L. Ibid. pp. 215-216.

11. MARCUTITZ, N. Ibid. pp. 271-273.

12. RAGAN, G.L. Ibid. pp. 372-373.

13. JASIK, H. 1961. Antenna Engineering Handbook. pp. 17/18 - 17/19.

14. GARDNER-FOX, A. 1947. An adjustable waveguide phase changer. Proc. IRE, December 1947, pp. 1489-1498.

15. RAGAN, G.L. Ibid. pp. 369-371.

16. RAGAN, G.L. Ibid. pp. 368-369.

17. TOMPKINS, R.D. 1956. A broad dual mode circular waveguide transducer. IRE Transactions on Microwave Theory and Techniques. 1956. pp. 181-183.

18. SILVER, S. Ibid. pp. 226-229.

19. JASIK, H. Ibid. pp. 30/18 - 30/19.

20. RAGAN, G.L. Ibid. pp. 367.

21. RAGAN, G.L. Ibid. pp. 336-338 and pp. 501-513.

22. RAGAN, G.L. Ibid. pp. 205-207.

23. RAGAN, G.L. Ibid. pp. 208.

24. RAGAN, G.L. Ibid. pp. 277-281.

25. YERUKHIMOVICH, Yu.A. 1973. Synthesis and analysis of optimal two-mirror antennas. Telecommunications and Radio Engineering (USA) – Vol. 28, part 2, Edition 7, pp. 82-89.

26. HANNAN, P.W. 1961. Microwave antennas derived from the Cassegrain telescope. IRE Transactions on Antennas and Propagation, 1961. pp. 140-153.

27. WILKINSON, E.J. *and* APPELBAUM, A.J. 1961. Cassegrain systems. IRE Transactions on Antennas and Propagation, 1961. pp. 119-120.

28. VIGGH, MATS. 1963. Designing for desired aperture illumination in Cassegrain antennas. Letters IEEE Transactions on Antennas and Propagation, 1963. pp. 1989199.

29. COLLINS, G.W. 1973. Shaping of subreflections in Cassegrain antennas for maximum aperture efficiency.

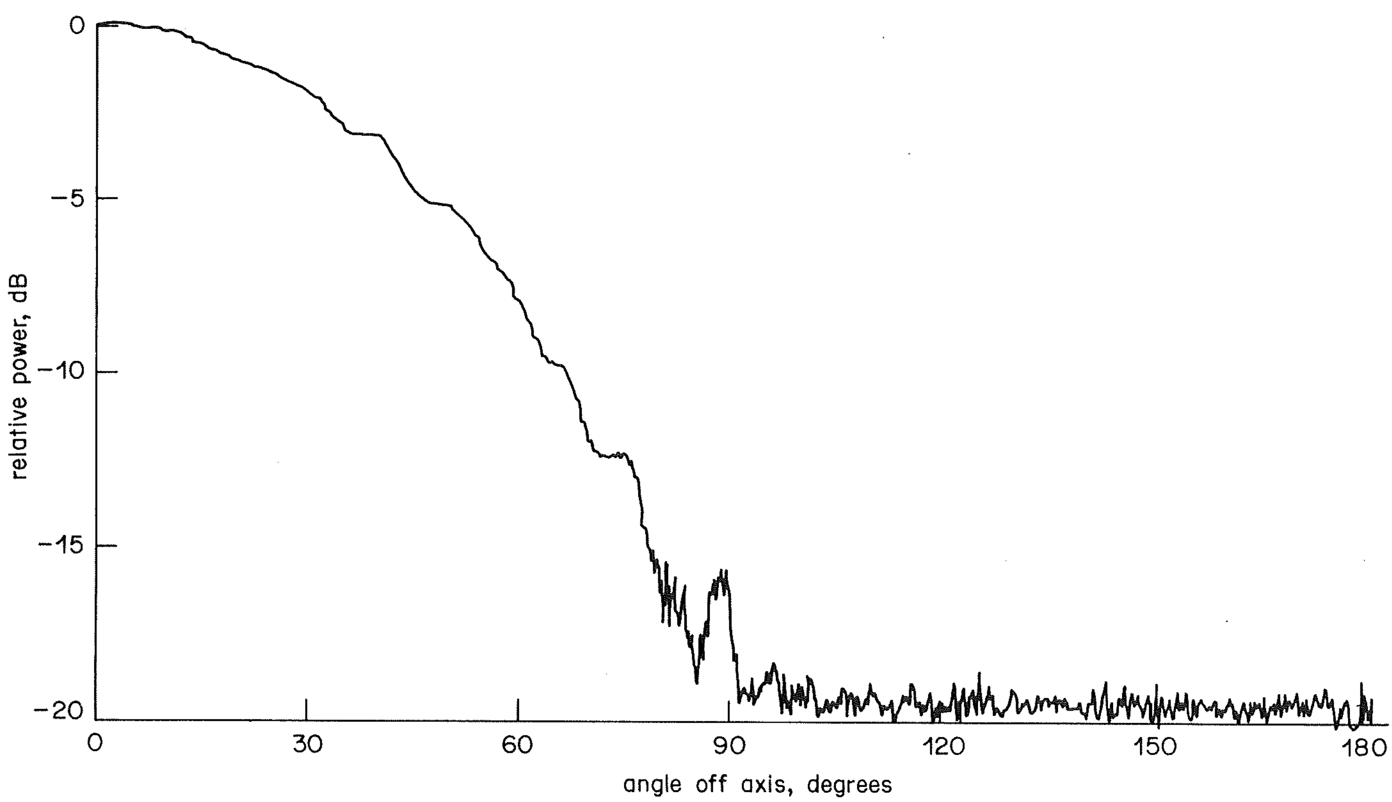

Fig. 13 - Feed aerial radiation pattern – H plane

IEEE transactions on Antennas and Propagation, 1973, Vol. AP-21, No. 3, pp. 309-313.

30. JASIK, H. Ibid. p. 12/6.

31. HAAS, Ludwig. 1975. Circularly-polarised pyramidal horns. Microwave Journal, 1975, Technical Note, pp. 30A-38C.

32. JASIK, H. Ibid. pp. 10/11-10/13.

33. SOUTHWORTH, G.C. 1939. Metal horns as directive receivers of ultra-short waves. Proceedings of the IRE, 1939, pp. 95-102.

34. JASIK, H. Ibid. pp. 30/20-30/21.

35. JASIK, H. Ibid. pp. 7/1 - 7/7.

36. JASIK, H. Ibid. p. 25/32.

37. JASIK, H. Ibid. p. 12/9.

38. WOHLLEBEN, R., WIELEBINSKI, R. *and* MATTES, H. 1971. Feeds for the 100 metre Effelsberg telescope. Proceedings of the 2nd European Microwave Conference, Stockholm, 1971, pp. 55/5:B5:4.

39. WOHLLEBEN, R. 1972. Simple small primary feed for large opening angles and high aperture efficiency. Electronics Letters, 1972. Vol. 8, No. li, pp. 474-476.

40. VU, T.B. *and* VU, Q H 1971. Corrugated Horns — recent developments. Proceedings of the 2nd European Microwave Conference, Stockholm, 1971, pp. B6/3:1 - B6/3:4.

41. NARASIMHAN, M.S. 1971. Corrugated conical horns with arbitary groove depth. Proceedings of the 2nd European Microwave Conference, Stockholm, 1971, pp. B6/4:1 - B6/4:6.

42. JASIK, H. Ibid. pp. 31/12-31/14.

43. RUDGE, A.W. *and* SHIRAZI, M. 1974. Investigation of reflector-antenna radiation — Final Report. Electrical Engineering Dept., Birmingham University.

44. SILVER, S. Ibid. pp. 443-446.

45. SILVER, S. Ibid. pp. 423.

46. FOLDES, P. 1972. A new earth-station antenna for domestic satellite communications. RCA Review, 1972, Vol. 33, pp. 695-728.

47. RAGAN, G.L. Ibid. pp. 218-223.

APPENDIX I

The relation between axial ratio and cross-polar isolation

An axial ratio R of 0 dB implies pure circular polarisation of one rotation sense, giving an infinite degree of isolation to the other, cross-polar, polarisation. However, an axial ratio of any other value implies that $E_y/E_x \neq 1$ so the polarisation is elliptical. This can be considered to consist of elements of both circular polarisations, thus:

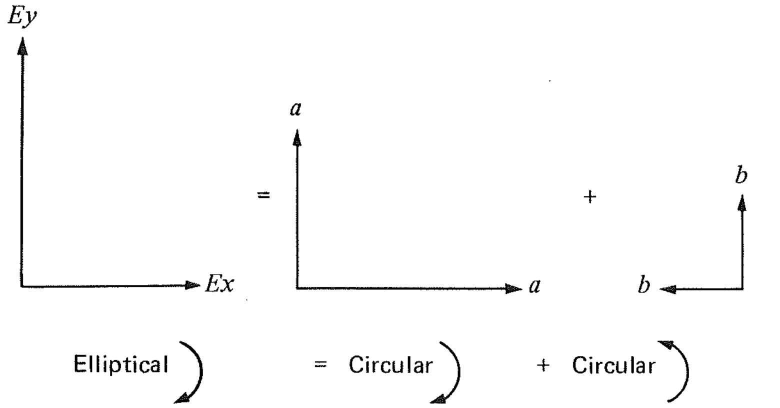

where $a = \frac{1}{2}(E_y + E_x)$ and $b = \frac{1}{2}(E_y - E_x)$

The axial ratio $R = 20 \log_{10} (E_y)/(E_x)$, so the relative powers in the two polarisations can be represented by the Isolation I, where

$$I = 20 \log_{10} \left(\frac{a}{b}\right) = 20 \log_{10} \left[\frac{\left(\text{alog}_{10} \dfrac{R}{20}\right) + 1}{\left(\text{alog}_{10} \dfrac{R}{20}\right) - 1}\right]$$

Example: If $R = 1{\cdot}5$ dB

then $$I = 20 \log_{10} \left[\frac{2{\cdot}19}{0{\cdot}19}\right] = 21{\cdot}28 \text{ dB}$$

HR/SB

Printed by BBC RESEARCH DEPARTMENT, Kingswood Warren, Tadworth, Surrey, KT20 6NP